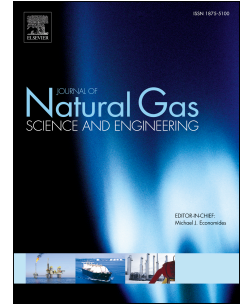


# Accepted Manuscript

Large-scale study of the effect of wellbore geometry on integrated reservoir-wellbore flow

Mohsen Azadi, Saïied M. Aminossadati, Zhongwei Chen



PII: S1875-5100(16)30579-0

DOI: [10.1016/j.jngse.2016.08.032](https://doi.org/10.1016/j.jngse.2016.08.032)

Reference: JNGSE 1729

To appear in: *Journal of Natural Gas Science and Engineering*

Received Date: 30 May 2016

Revised Date: 22 July 2016

Accepted Date: 11 August 2016

Please cite this article as: Azadi, M., Aminossadati, S.M., Chen, Z., Large-scale study of the effect of wellbore geometry on integrated reservoir-wellbore flow, *Journal of Natural Gas Science & Engineering* (2016), doi: 10.1016/j.jngse.2016.08.032.

This is a PDF file of an unedited manuscript that has been accepted for publication. As a service to our customers we are providing this early version of the manuscript. The manuscript will undergo copyediting, typesetting, and review of the resulting proof before it is published in its final form. Please note that during the production process errors may be discovered which could affect the content, and all legal disclaimers that apply to the journal pertain.

1 **Large-Scale Study of the Effect of Wellbore Geometry on**  
2 **Integrated Reservoir-Wellbore Flow**

3 Mohsen Azadi\*, Saeed M. Aminossadati, Zhongwei Chen

4 *School of Mechanical and Mining Engineering, The University of Queensland, Brisbane, Queensland 4072,*

5 *Australia*

---

\* Corresponding author at: School of Mechanical and Mining Engineering, The University of Queensland, QLD 4072, Australia. Tel.: +61 7 33653676; fax: +61 7 33653888.  
E-mail address: mohsen.azadi@uq.edu.au (Mohsen Azadi)

**1 Abstract:**

2 Extraction of coal seam gas (CSG) prior to mining is crucial for reducing the potential risks  
3 of gas outburst and explosions during underground coal mining as well as gas production  
4 purposes. Many numerical and experimental studies have been carried out to identify the  
5 factors affecting the gas productivity. These factors include coal properties, gas content and  
6 wellbore geometries. Two different flow conditions determine the gas production efficiency:  
7 The gas flow inside the wellbore injected from wall, and the flow through porous coal  
8 medium. The full understanding of simultaneous flow of fluids through reservoir and  
9 wellbore is critical for analysing the reservoir behaviour. However, previous studies  
10 examined the flow of these fluids separately. In this research, a large scale three-dimensional  
11 model for simulation of integrated reservoir-wellbore flow is developed to study the effect of  
12 wellbore geometry on flow characteristics and wellbore productivity. Four different wellbore  
13 diameters of 0.075, 0.10, 0.125 and 0.15 *m* as well as three different lengths of 50, 100, and  
14 150 *m* were chosen to accomplish the parametric study of wellbore geometry. It is assumed  
15 that the wellbores were in a steady-state condition for two different single phase scenarios of  
16 water and methane gas flow. The simulation results were validated against the pressure drop  
17 models for internal single phase gas and water flow reported in the literature. The obtained  
18 results revealed that increasing the wellbore diameter led to reduction of fluid pressure in the  
19 coal seam. Regarding the effect of wellbore length, it was observed that at a specific distance  
20 from wellbore outlet, the pressure distribution is independent of the wellbore length and  
21 upstream effects. It is also shown that wellbore production could be enhanced by increasing  
22 the diameter and the length of wellbore for both gas and liquid flow. The developed  
23 integrated framework can be used further for study of any enhanced gas recovery method by  
24 changing the boundary conditions based on the physical model.

25 *Keywords:* Reservoir; Wellbore; Coal Seam Gas; Productivity Index; CFD

**1 Nomenclature**

- 2 D wellbore diameter,  $m$   
3 L wellbore length,  $m$   
4  $g$  gravitational acceleration,  $m/s^2$   
5  $h$  reservoir thickness,  $m$   
6  $J_D$  dimensionless productivity index  
7  $k$  reservoir permeability,  $m^2$   
8  $q$  volumetric production rate,  $m^3/s$   
9  $P$  pressure,  $Pa$   
10  $S_i$  momentum sink term,  $kg/m^2s^2$   
11  $S_m$  mass source term,  $kg/m^3s$   
12  $V$  velocity,  $m/s$   
13  $x,y,z$  cartesian coordinates,  $m$

14

15 *Greek letters*

- 16  $\mu$  dynamic viscosity,  $Pa s$   
17  $\rho$  density,  $kg/m^3$   
18  $\tau$  shear stress,  $Pa$

19

20 *Subscript*

- 21 0 reference values  
22  $g$  gas phase  
23  $l$  liquid phase  
24  $w$  wellbore

25

## 1 **1. Introduction**

2 Coal seams naturally contain a large amount of gases such as methane (CH<sub>4</sub>) and carbon-  
3 dioxide (CO<sub>2</sub>). In a general estimation, the gas content for different types of coal varies  
4 between 0.1 and 25 m<sup>3</sup> per tonne of coal. Coal seam gas (CSG) is mainly composed of  
5 methane (CH<sub>4</sub>), which is estimated at 80%-95% of overall gas content. There are still many  
6 technical challenges associated with gas production from deep coal seams with high gas  
7 content and low permeability. In order to overcome these challenges, wellbores are  
8 commonly drilled directionally from vertical to horizontal sections with different diameter  
9 and lengths. A reliable prediction of CSG flow depends on the appropriate consideration of  
10 coal structure and reservoir properties as well as production wellbore geometry. Previous  
11 investigations of CSG production has been focused mainly on either reservoir simulations or  
12 wellbore flow characteristics.

13 Many studies have been carried out to simulate flow of fluids from different types of  
14 reservoirs into wellbores (Jenkins and Aronofsky, 1953; Aronofsky and Jenkins, 1954; Al-  
15 Hussainy, et al., 1966; Yao, et al., 2013). Early theoretical models or numerical simulations  
16 were developed primarily for oil and gas applications. Jenkins and Aronofsky (1953)  
17 presented a numerical method for describing the transient flow of gases in a radial direction  
18 through a porous medium for which the initial and terminal pressure and/or flow rates are  
19 specified. They developed a simple means for predicting the well pressure at any time in the  
20 history of a reservoir. In their next study (Aronofsky and Jenkins, 1954) an effective drainage  
21 radius was suggested for which the steady-state gas flow assumption could be used to predict  
22 the well pressure in the process of gas reservoir depletion. In a rigorous model, Al-Hussainy  
23 et al. (1966) considered the effect of variations of pressure dependent viscosity and gas law  
24 deviation factor on the flow of real gases through porous media. They used pseudo-pressure  
25 as change of variable to reduce the equations to a form similar to diffusivity equations. Yi et

1 al. (2009) simulated gas flow through a reservoir using a two-dimensional solid-gas coupled  
2 software package (RPFA). They studied the effect of permeability, wellbore spacing and  
3 diameter and gas content on reservoir pressure and drainage radius. Packman et al. (2011)  
4 used SimedWin to simulate CSG flow in an attempt to demonstrate the ability of enhanced  
5 gas recovery. Based on their reservoir model calibrated by history matching, they concluded  
6 that with regard to increased gas flow rate and decreased drainage time, enhanced gas  
7 recovery through injection of nitrogen is achievable. Most of these researches have focused  
8 only on reservoir aspects of simulation and their assumptions, such as defined boundary  
9 conditions at wellbore and one- or two-dimensional, require further improvements in terms of  
10 flow dimensions. The errors associated with the simplifying assumptions limit the range of  
11 application of these reservoir simulators. Moreover, the wellbore flow is defined as a  
12 boundary condition and is not included in the mathematical modelling and governing  
13 equations of the reservoir simulators. These assumptions neglected the interactions between  
14 the reservoir and wellbore interfaces.

15 On the effect of wellbore wall influx/outflux, a number of studies have been carried out to  
16 understand the flow filed behaviour and pressure drop along wellbores (Asheim, et al., 1992;  
17 Yuan, 1997; Su and Gudmundsson, 1998; Yuan, et al., 1999). Siwon (1987) developed a one-  
18 dimensional model for steady state flow of incompressible fluid in a horizontal pipe  
19 perforated with circular orifices. Ouyang et al. (1998) continued this study by developing a  
20 pressure drop model for pipes with perforated wall that can easily be used in reservoir  
21 simulators and analytical models. This model considers different types of pressure drops  
22 including frictional, accelerational, gravitational and pressure drop caused by inflow. They  
23 concluded that for laminar flow, the wall friction increases due to inflow whereas for  
24 turbulent flow, the wall friction decreases as a result of inflow. Based on this approach, more  
25 attempts have been made to develop the most accurate pressure drop models for wellbore

1 flow. Yalniz and Ozkan (2001) investigated the effect of inflow from horizontal wall on flow  
2 characteristics and pressured drop experimentally and theoretically. They developed a  
3 generalized friction factor correlation that was a function of Reynolds number, the ratios of  
4 influx to wellbore flow rate and perforations to wellbore diameter. Wang et al. (2011)  
5 measured pressure drop due to inflow in a horizontal perforated pipe loop by using water as  
6 working fluid. Their experimental results showed that pressure drop grew as a result of  
7 increased injection flow rate. They developed a model suggesting total pressure drop  
8 consisting of two parts including perforated pipe wall friction loss and an additional pressure  
9 drop term. In a recent study, Zhang et al. (2014) presented a comprehensive model for  
10 prediction of pressure drop based on previous studies and some new experiments. Their  
11 results show that this model presents more accurate results for their experiments when  
12 compared with previous models.

13 In addition to theoretical models, some researchers have simulated wellbore flow using  
14 numerical techniques to avoid the simplifying assumption (Folefac et al., 1991; Seines et al.,  
15 1993; Siu, et al., 1995; Su and Lee, 1995; Yuan, et al., 1998; Ouyang and Huang, 2005). Guo  
16 et al. (2006) developed a numerical model to study the deliverability of multilateral wells.  
17 Their model was capable of coupling the inflow performance of the individual laterals with  
18 hydraulics in curved and vertical well sections. Zeboudj and Bahi (2010) simulated wellbore  
19 flow with pipe injection using Computational Fluid Dynamics (CFD) simulation as a  
20 replacement for further experiments. They discussed the experimental measurement  
21 shortcoming in the assumption of a constant momentum-correction factor, which was not true  
22 in the case of wall inflow. CFD simulation, however, allowed the exact calculation of this  
23 parameter by considering all variations of velocity in radial direction by eliminating the need  
24 for making flawed assumptions. In another study, Ouyang et al. (2009) studied single-point  
25 wall entry for oil and gas wellbores. The significant effect of wellbore hydraulics on

1 production predictions, performance evaluations and completion design for horizontal and  
2 multilateral wellbores needed to be well understood. In this respect, they used CFD  
3 modelling using ANSYS to investigate flow profiles and pressure distribution along the  
4 wellbore thoroughly. Their simulation results showed that moving the entry point closer to  
5 the outlet section reduced the significant impact of inflow on the total pressure drop along the  
6 wellbore.

7 Depending on wellbore geometry, the flow characteristics through the coal seam and  
8 wellbore may vary significantly. Some theoretical models and reservoir simulators have been  
9 presented accordingly. However, these models need further improvements with regard to the  
10 simplification of boundary condition assumptions on the reservoir-wellbore interface.  
11 Efficient production of coal seams gas requires a better understanding of reservoir and  
12 wellbore conditions and their interactions. In this study, a large-scale three-dimensional  
13 model is developed using CFD simulations to study the integrated reservoir-wellbore flow  
14 during CSG production. The specific influence of wellbore diameter and length on the coal  
15 seam flow behaviour, pressure drop and production performance is investigated. A schematic  
16 of reservoir-wellbore model with assumed boundary conditions is presented in Fig. 1.

17

## 18 **2. Mathematical modelling**

### 19 *2.1. Model assumptions*

20 CSG is trapped inside the coal seam by water and ground pressure. The methane gas is  
21 maintained inside the coal matrix sealed with water existing in coal fractures (i.e. cleats). As  
22 the reservoir pressure at wellbore reduces, the water begins to flow out of cleats letting the  
23 gas be desorbed from the coal matrix. Based on the described production process, the  
24 following assumptions have been taken into consideration:



- 1       ▪ Water is considered as the working fluid for the single phase liquid flow;
- 2       ▪ Methane (a compressible ideal gas) is considered as the working fluid for the single
- 3       phase gas flow;
- 4       ▪ The simulations are conducted in the single phase production phase and in the steady
- 5       state condition;
- 6       ▪ Two cell zone conditions for porous coal seam and internal wellbore flow are
- 7       considered;
- 8       ▪ Coal is considered as a homogenous porous media holding gas in the coal matrix;
- 9       ▪ Fluid flow through the fracture network of coal obeys Darcy's law;
- 10      ▪ Flow through the wellbore is considered turbulent; and
- 11      ▪ The flow variables are transferred between wellbore and porous zone by defining an
- 12      interface at the contact region of the two zones.

13 One of the most determining parameters, affecting gas production from coal seams, is the  
14 coal (reservoir) permeability. Coal permeability varies from near 0.1 to 100 *md* for deep and  
15 shallow reservoirs, respectively (Darling, 2011). In this study, the horizontal and vertical  
16 permeability of 10 *md* and 1 *md*, respectively, are considered for the coal seam zone. In order  
17 to generalize the computed results, the dimensionless parameters, given in Table 1, are  
18 defined. The reference values of  $D_0=0.1\text{ m}$ ,  $L_0=100\text{ m}$ ,  $P_0=1\text{ atm}$ ,  $\rho_{0,l}=998.2\text{ kg/m}^3$ ,  $\rho_{0,g}=0.67$   
19  $\text{kg/m}^3$  are assumed for wellbore diameter, length, pressure, liquid density and gas density,  
20 respectively.

21

## 22 2.2. Governing equations

23 Based on the mentioned assumptions two different sets of equations are required to simulate  
24 flow through the wellbore and coal seam. Flow in the wellbore section is considered as

1 internal turbulent pipe flow with distributed mass transfer through the wall, and flow through  
 2 the coal seam is treated as a porous media flow.

3

4

### 5 2.2.1. Wellbore flow equations

6 Considering varying mass transfer across reservoir-wellbore intersection, the conservation  
 7 equations of mass momentum and energy can be written as follows:

$$\frac{\partial}{\partial x_i}(\rho u_i) = 0 \quad (1)$$

$$\frac{\partial}{\partial x_j}(\rho u_i u_j) = -\frac{\partial P}{\partial x_i} + \frac{\partial}{\partial x_j} \left[ \mu \left( \frac{\partial u_i}{\partial x_j} + \frac{\partial u_j}{\partial x_i} - \frac{2}{3} \delta_{ij} \frac{\partial u_l}{\partial x_l} \right) \right] + \frac{\partial \tau_{ij}}{\partial x_j} + \rho \bar{g} \quad (2)$$

8 where  $\tau_{ij}$  is the Reynold stress tensor that represents the effect of turbulent fluctuations on  
 9 fluid flow and is defined by:

$$\tau_{ij} = -\overline{\rho u_i u_j} \quad (3)$$

10 This term is computed using standard  $k - \varepsilon$  turbulence models to close the mass and  
 11 momentum equations. This turbulent model has been widely used and verified for simulation  
 12 of wellbore flow with wall injection by a number of previous studies (Su, 1996; Yuan, 1997;  
 13 Ouyang et al., 2009). The details of turbulence models used in the current study with all the  
 14 constant values can be found in theory guide of the software package (FLUENT, 2011).

15

### 16 2.2.2. Reservoir flow equations

1 The volume blockage, which is physically present, is not represented in the model. Therefore,  
 2 a superficial velocity inside the porous medium based on the volumetric flow rate is used.  
 3 This is to ensure the continuity of velocity vectors across the porous medium interface. The  
 4 porous medium is modelled by the addition of a momentum sink term to the standard fluid  
 5 flow equations. To do this, Darcy's flow is considered through the coal fracture network.  
 6 Under the suggested assumptions for coal seam zone, the conservation equations are written  
 7 below:

$$\frac{\partial}{\partial x_i}(\rho u_i) = S_m \quad (4)$$

$$\frac{\partial}{\partial x_j}(\rho u_i u_j) = -\frac{\partial P}{\partial x_i} + \frac{\partial}{\partial x_j} \left[ \mu \left( \frac{\partial u_i}{\partial x_j} + \frac{\partial u_j}{\partial x_i} - \frac{2}{3} \delta_{ij} \frac{\partial u_l}{\partial x_l} \right) \right] + \frac{\partial \tau_{ij}}{\partial x_j} + \rho \bar{g} + \bar{S}_i \quad (5)$$

8 where  $S_m$  is the mass source term accounting for the production of gas from coal seam. In  
 9 order to add mass source term in reservoir zone, internal functions and macros supplied by  
 10 ANSYS Fluent are compiled in the C programming language and then hooked to the solver.  
 11 The macro used in this study, specifies the custom mass source term  $S_m$  in Eq. (4) at each cell  
 12 across the reservoir with units of  $kg/m^3s$ . The last term in Eq. (5) is defined using Darcy's  
 13 Law:

$$\bar{S}_i = -\frac{\mu}{k} \bar{v}_i \quad (6)$$

14 The above momentum sink term contributes to the pressure gradient in the porous cell,  
 15 creating a pressure drop that is proportional to the fluid velocity in the cell.

16

### 17 2.3. Implementation of computational model

18 A section of horizontal wellbore is chosen as the base physical model. A  $100 \times 5$  m coal panel  
 19 with seam thickness of 2.5 m and a wellbore diameter of 0.1 m is considered as the baseline

1 condition. Outlet atmospheric pressure boundary condition is applied at the wellbore end.  
2 Four different wellbore diameters of 0.075, 0.1, 0.125 And 0.15  $m$  as well as three different  
3 lengths of 50, 100, and 150  $m$  are chosen to accomplish the parametric study of wellbore  
4 geometry. The Semi-implicit Method Pressure-linked Equations (SIMPLE) algorithm is used  
5 for the pressure–velocity coupling. The second-order upwind discretization scheme is utilized  
6 for the momentum, turbulent kinetic energy, and turbulent dissipation rate. The computations  
7 are carried out using parallel processing on a high performance computing workstation with  
8 32 nodes. Each node is configured as follows:  $2 \times 10$  cores @2.60GHz, 128GB RAM.

### 9 **3. Results and discussion**

#### 10 *3.1. Grid convergence and model validation*

11 The computational meshes with high resolution of approximately 1.5 million hexahedral cells  
12 were generated with ANSYS Meshing. The average orthogonal quality of 93.2% with  
13 standard deviation of 4.8% was achieved for the generated grid. Due to higher pressure  
14 gradient at the reservoir-wellbore interface, finer meshes were created near the interface to  
15 capture sudden flow variations as presented in Fig. 2. In order to study the grid-independency  
16 of simulations, pressure drop along wellbores with different diameters were plotted for three  
17 meshes with coarse, medium and fine resolutions as shown in Fig. 3. It is seen that using a  
18 higher mesh resolution does not influence the simulation results confirming that a grid-  
19 independent solution is achieved.

20 The simulations are conducted for both methane flow and water flow as the working fluids  
21 during the fluid production from underground coal seams. The computed results for methane  
22 flow along the wellbore are compared with Atkinson's equation (Le Roux, 1990) to  
23 determine the pressure drop using the following equation:

$$\Delta P = \frac{C P_{er} L}{A^3} \frac{\rho}{\rho_{air}} Q^2 \quad (7)$$

1 where  $\Delta P$  is the pressure drop ( $Pa$ ),  $C$  is Atkinson friction factor ( $kg/m^3$ ),  $P_{er}$  is wellbore  
 2 perimeter ( $m$ ),  $A$  is cross-sectional area ( $m^2$ ),  $\rho$  is gas density ( $kg/m^3$ ), and  $Q$  is gas  
 3 flow rate ( $m^3/s$ ). The computed pressure drops for four different diameters (coloured with  
 4 diameters) as well as three different lengths are presented in Fig. 4. The simulation results  
 5 show good agreement with Atkinson's equation. For the water flow, the simulation results are  
 6 compared with the following pressure drop model along the pipes (Aziz and Govier, 1972):

$$\Delta P = 2f \frac{\rho V^2 L}{D} \quad (8)$$

$$f = \begin{cases} \frac{16}{Re} & \text{for } Re \leq 2200 \\ 0.077716 \left\{ \log \left[ \frac{6.9}{Re} + \left( \frac{\varepsilon}{3.7D} \right)^{1.11} \right] \right\}^{-2} & \text{for } Re > 2200 \end{cases} \quad (9)$$

7 where  $Re$  is the Reynold number,  $\varepsilon$  is the absolute pipe roughness. Same geometries as  
 8 described for methane flow are now used for water flow (Figure 5). It can be seen that the  
 9 results are in good agreement with the pressure drop model along pipes.

10 In order to evaluate the integrated reservoir-wellbore model performance, more simulations  
 11 were carried out for the case of wellbore-only flow with wall inflow. Velocity inlet with  
 12 uniform distribution normal to wellbore pipe was defined at wellbore wall to account for  
 13 methane gas flowing from upstream reservoir. The pressure drop results for the wellbore  
 14 model is compared with presented integrated reservoir-wellbore model and Atkinson's  
 15 equation in Table 2. It is seen that the integrated model provides more accurate results  
 16 compared to wellbore flow model. A close examination of the velocity vectors at the  
 17 reservoir-wellbore interface for the integrated model shows that the gas is released into the  
 18 wellbore in the direction of wellbore stream. However, the wellbore-only model

1 overestimation can be explained by normal direction of wall inflow to main stream and  
2 consequently higher pressure drop for accelerating the injected fluid.

3 The velocity streamlines through coal seam and wellbore are illustrated in Figure 6. As  
4 presented in this figure, fluid motion originates from coal seam under the influence of large  
5 pressure gradient near the wellbore. It was observed that fluid velocity grows sharply as  
6 travelling across the reservoir and towards the wellbore. The presented flow mechanism  
7 proves the important influence of efficient wellbore drilling on reservoir production.  
8 Development of a three-dimensional integrated model can be considered as a promising tool  
9 to improve our understandings about flow field variables and behaviour. These results are  
10 essential for advancement of wellbore development plans and study of improved fluid  
11 recovery methods where few in-situ data are available due to access limitations and  
12 geometrical difficulties. The presented reservoir-model is further evaluated by two parametric  
13 studies on the effect of wellbore geometry and length in the following sections.

### 14 15 *3.2. Effect of wellbore diameter*

16 Pressure contours at five planes ( $x^*=0, 0.25, 0.5, 0.75, 1$ ) along and three planes ( $z^*=-25, 0,$   
17  $25$ ) across the coal seam for single phase flow of gas and water are illustrated in Fig. 7. It is  
18 evident that by increasing the wellbore diameter, the fluid pressure throughout the coal seam  
19 decreases. Development of larger wellbores lead to larger production area across the reservoir  
20 as well as lower pressure drop and flow resistance along the wellbores. As a result, the model  
21 confirms that gas production can be enhanced by development of larger diameter wellbores.

22 To scrutinise the effect of wellbore diameter on coal seam pressure distribution, the pressure  
23 profiles in a vertical direction across the coal seam at  $x^*=0.5$  are plotted (Figure 8). It is  
24 observed that the flow pressure increases sharply and reaches approximately a constant value

1 as moving away from the wellbore to the coal seam in a vertical direction. Comparison of  
2 different diameter curves shows that larger diameter wellbores are more effective in reducing  
3 the reservoir pressure and higher production.

4 Velocity profiles for four different wellbore diameters along the wellbore centreline for  
5 methane and water flow are presented in Fig. 9. The velocity magnitude varies inversely with  
6 wellbore diameter to satisfy the continuity of mass flow rate at the wellbore outlet for similar  
7 fluid production from the reservoir. The velocity grows almost linearly moving from the  
8 wellbore toe to the heel as the fluid is injected from the wall to the main stream. The velocity  
9 profile along a vertical direction at three different sections along wellbore ( $x^*=0, 0.5, 1$ ) for  
10 methane and water flow are presented in Fig. 10. Comparison of velocity profiles at  
11 reservoir-wellbore interface shows that the integrated model has captured the sudden velocity  
12 increase as moving from reservoir to wellbore. It is also evident that moving from coal seam  
13 end to outlet section, the velocity magnitude increases considerably due to continuous  
14 injection of fluid along the wellbore.

15

### 16 *3.3. Effect of wellbore length*

17 Pressure contours for different wellbore lengths at three planes with similar distance of 0, 25,  
18 50 m from wellbore outlet and three planes ( $z^*=-25, 0, 25$ ) across the coal seam for single  
19 phase methane flow are presented in Fig. 11. These three planes along the wellbore are  
20 chosen to investigate the influence of upstream effects on production behaviour and pressure  
21 distribution through coal seams with longer wellbores. Pressure through the coal seam in the  
22 far from wellbore regions does not vary significantly along the coal seam in the  $x$  direction.  
23 This behaviour can be explained by the greater value of coal permeability in the horizontal  
24 plane compared to the vertical plane. The pressure contours for the three cases show that for a

1 specific distance from the wellbore outlet, the pressure distribution is almost independent of  
 2 wellbore length and upstream effects.

3 This observation is investigated further by studying pressure profiles across the horizontal  
 4 and vertical directions through coal seams of different lengths ( $x^*=0.5, 1, 1.5$ ) as presented in  
 5 Fig. 12. As can be seen, at a similar distance from the wellbore outlet, the upstream wellbore  
 6 flow does not influence pressure distribution across the reservoir. The pressure increases  
 7 more sharply when moving away from the wellbore in the  $y$  direction due to higher  
 8 permeability in vertical plane compared to horizontal plane. Velocity profiles across the  
 9 vertical direction at a distance of 25 m from the wellbore outlet for three different coal seam  
 10 lengths ( $x^*=0.5, 1, 1.5$ ) are presented in Fig. 13. It is evident that the longest coal seam has  
 11 the highest velocity magnitude across the wellbore which can be explained by the higher  
 12 injection from upstream reservoir to the wellbore. Similar observations, presented in Figs. 11-  
 13 13, are observed for the effect of wellbore length on single phase water flow through coal  
 14 seam and wellbore.

#### 16 3.4. Effect of wellbore geometry on productivity index

17 One of the appropriate tools for evaluating the wellbore performance in petroleum  
 18 engineering is productivity index (PI) which is defined as the ratio of produced liquid flow  
 19 rate to pressure drawdown. In order to study the effect of wellbore geometry on wellbore  
 20 performance, dimensionless productivity index ( $J_D$ ) is calculated as follows:

$$J_D = \frac{\mu}{2\pi kh} \times \frac{q}{\bar{P} - P_w} \quad (10)$$

21 The effect of wellbore diameter and length on productivity index for the single phase methane  
 22 flow and water flow is presented in Fig. 14. Regarding the impact of wellbore diameters, the  
 23 CFD results show that increasing the diameters leads to higher PI which is consistent with



1 previous findings. Similar behaviour is observed on the effect of wellbore length considering  
2 greater production volume for longer reservoir sections. The presented simulations and case  
3 studies verifies the improved capability of the current integrated reservoir-wellbore model as  
4 a promising tool for further studies of enhanced fluid recovery.

5

#### 6 **4. Conclusions**

7 A three-dimensional CFD model for the simulation of integrated reservoir-wellbore flow is  
8 developed to study the significant effect of wellbore geometry on flow characteristics of coal  
9 seams. Four different wellbore diameters and three lengths are simulated for single phase  
10 methane and water flow. The numerical simulation results show that by increasing the  
11 wellbore diameters the fluid pressure throughout the coal seam falls, resulting in more  
12 efficient production from coal seam. It can also be seen that the velocity magnitude is  
13 remarkably larger across wellbore than through reservoir and moving from coal seam end to  
14 outlet section, the velocity magnitude increases considerably due to continuous injection of  
15 fluid along the wellbore. Pressure distribution through the coal seam in the far from wellbore  
16 regions does not vary significantly along the wellbore due to higher permeability of porous  
17 media in horizontal plane. In addition, the computational results indicate that for a specific  
18 distance from the wellbore outlet, the pressure distribution is almost independent of wellbore  
19 length and upstream effects. It is confirmed that with increasing the wellbore diameters and  
20 lengths the wellbore productivity index is enhanced. This study proves that the presented  
21 CFD model can be used as a promising tool for study of wellbore performance predictions as  
22 well as enhanced fluid recovery methods. This model can provide the engineers with in-situ  
23 data using an inexpensive and flexible computer model.

24

## 1   **References**

- 2   Al-Hussainy, R., H. Ramey Jr and P. Crawford (1966). "The flow of real gases through  
3   porous media." *Journal of Petroleum Technology* **18**(05): 624-636.
- 4   Aronofsky, J. and R. Jenkins (1954). "A simplified analysis of unsteady radial gas flow."  
5   *Journal of Petroleum Technology* **6**(07): 23-28.
- 6   Asheim, H., J. Kolnes and P. Oudeman (1992). "A flow resistance correlation for completed  
7   wellbore." *Journal of Petroleum Science and Engineering* **8**(2): 97-104.
- 8   Aziz, K. and G. W. Govier (1972). *The Flow of Complex Mixtures in Pipes* [by] GW Govier  
9   and K. Aziz, New York: Van Nostrand Reinhold Company.
- 10   Darling, P. (2011). *SME Mining Engineering Handbook*. Littleton, SME.
- 11   Fluent, A. (2011). "Ansys Fluent Theory Guide." ANSYS Inc., USA.
- 12   Folefac, A. N., J. S. Archer, R. I. Issa and A. M. Arshad (1991). *Effect of Pressure Drop  
13   Along Horizontal Wellbores on Well Performance*, Society of Petroleum Engineers.
- 14   Guo, B., K. Ling and A. Ghalambor (2006). *A Rigorous Composite-IPR Model for  
15   Multilateral Wells*, Society of Petroleum Engineers.
- 16   Jenkins, R. and J. Aronofsky (1953). "Unsteady radial flow of gas through porous media."  
17   *Journal of Applied Mechanics-Transactions of the ASME* **20**(2): 210-214.
- 18   Le Roux, W. (1990). *Le Roux's Notes on Mine Environmental Control, Mine Ventilation  
19   Society of South Africa*.
- 20   Ouyang, L.-B., S. Arbabi and K. Aziz (1998). "General Wellbore Flow Model for Horizontal,  
21   Vertical, and Slanted Well Completions."
- 22   Ouyang, L.-B. and W. S. B. Huang (2005). *A Comprehensive Evaluation of Well-  
23   Completion Impacts on the Performance of Horizontal and Multilateral Wells*, Society of  
24   Petroleum Engineers.

- 1 Ouyang, L. C., D. Sun and L. B. Ouyang (2009). "Numerical Investigation of the Impacts of  
2 Wall Fluid Entry on Fluid Flow Characteristics and Pressure Drop along a Wellbore."  
3 *Petroleum Science and Technology* **27**(18): 2109-2133.
- 4 Packham, R., Y. Cinar and R. Moreby (2011). "Simulation of an enhanced gas recovery field  
5 trial for coal mine gas management." *International Journal of Coal Geology* **85**(3–4): 247-  
6 256.
- 7 Seines, K., I. Aavatsmark, S. C. Lien and P. Rushworth (1993). "Considering wellbore  
8 friction effects in planning horizontal wells." *Journal of Petroleum Technology; (United*  
9 *States); Journal Volume: 45:10: Medium: X; Size: Pages: 994-1000.*
- 10 Siu, A., D. Shin and G. Subramanian (1995). *A Complete Hydraulics Model for Horizontal*  
11 *Wells, Society of Petroleum Engineers.*
- 12 Siwoń, Z. (1987). "Solutions for Lateral Inflow in Perforated Conduits." *Journal of Hydraulic*  
13 *Engineering* **113**(9): 1117-1132.
- 14 Su, Z. (1996). "Pressure drop in perforated pipes for horizontal wells", Norwegian  
15 University of Science and Technology, Trondheim, Norway.
- 16 Su, H. J. and S. H. Lee (1995). "Modeling Transient Wellbore Behavior in Horizontal Wells",  
17 *Society of Petroleum Engineers.*
- 18 Su, Z. and J. S. Gudmundsson (1998). "Perforation inflow reduces frictional pressure loss in  
19 horizontal wellbores." *Journal of Petroleum Science and Engineering* **19**(3–4): 223-232.
- 20 Wang, Z., J. Xiao, X. Wang and J. Wei (2011). "Experimental study for pressure drop of  
21 variable mass flow in horizontal well." *J. Exp. Fluid Mech* **25**(5): 26-29.
- 22 Yalniz, M. U. and E. Ozkan (2001). "A Generalized Friction-Factor Correlation To Compute  
23 Pressure Drop in Horizontal Wells."
- 24 Yao, S., F. Zeng, H. Liu and G. Zhao (2013). "A semi-analytical model for multi-stage  
25 fractured horizontal wells." *Journal of Hydrology* **507**: 201-212.

- 1 Yi, L.-j., Z.-l. Tang and Q.-x. Yu (2009). Computer simulation of gas pressure and drainage  
2 radius for dense wellbores gas pre-drainage in outburst coal seam. *Computer Science &*  
3 *Education*, 2009. ICCSE '09. 4th International Conference on.
- 4 Yuan, H. (1997). Investigation of single phase liquid flow behavior in horizontal wells, in,  
5 University of Tulsa, 1997.
- 6 Yuan, H., C. Sarica and J. P. Brill (1998). Effect of Completion Geometry and Phasing on  
7 Single-Phase Liquid Flow Behavior in Horizontal Wells, Society of Petroleum Engineers.
- 8 Yuan, H. J., C. Sarica and J. P. Brill (1999). "Effect of Perforation Density on Single-Phase  
9 Liquid Flow Behavior in Horizontal Wells."
- 10 Zeboudj, F. and L. Bahi (2010). Horizontal Well Performance Flow Simulation CFD-  
11 Application, Society of Petroleum Engineers.
- 12 Zhang, Q., Z. Wang, X. Wang and J. Yang (2014). "A New Comprehensive Model for  
13 Predicting the Pressure Drop of Flow in the Horizontal Wellbore." *Journal of Energy*  
14 *Resources Technology* **136**(4): 042903-042903.

15

16

**1 Figure Captions**

2 Fig. 1 – A schematic diagram of reservoir-wellbore model

3 Fig. 2 – Computational mesh of reservoir-wellbore model

4 Fig. 3 – Pressure drop vs. wellbore diameter for methane flow with different mesh resolutions

5 Fig. 4 – Comparison of simulated model for methane flow with Atkinson equation (Le Roux,  
6 1990)

7 Fig. 5 – Comparison of simulated model for water flow with (Aziz and Govier, 1972)  
8 correlation

9 Fig. 6 – Velocity streamlines through coal seam reservoir and wellbore

10 Fig. 7 – Pressure contours along coal seam for different wellbore diameters for: a) methane  
11 flow, and b) water flow

12 Fig. 8 – Pressure distribution in y direction across coal seam at  $x^*=0.5$  for: a) methane flow,  
13 and b) water flow

14 Fig. 9 – velocity along wellbore centreline for: a) methane flow, and b) water flow

15 Fig. 10 – Velocity profile along Y direction for methane (left) and water (right) flow at: a,c)  
16  $x^*=0$ ; b,d)  $x^*=0.5$ ; e,f)  $x^*=1$

17 Fig. 11 – Pressure contours along coal seam for different wellbore lengths

18 Fig. 12 – Pressure distribution at distance of 25 m from wellbore outlet in: a) y direction, and  
19 b) z direction

20 Fig. 13 – Velocity profile along y direction at the distance of 25 m from wellbore outlet for  
21 different wellbore lengths

1 Fig. 14 – Productivity index for different wellbore geometries. a) wellbore diameter; b)  
2 wellbore lengths

3

4 **Table caption**

5 Table 1. Dimensionless parameters

6 Table 2. Comparison of wellbore-only model with integrated reservoir-wellbore model

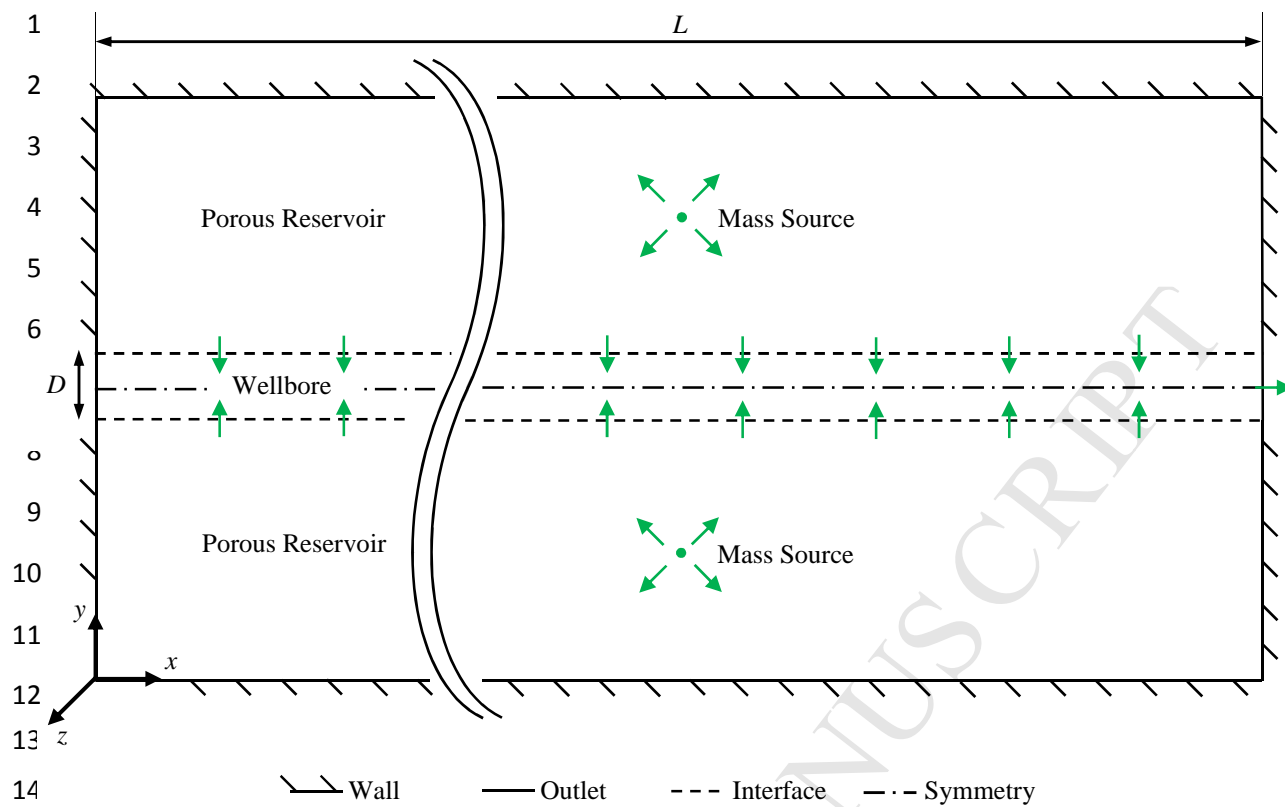
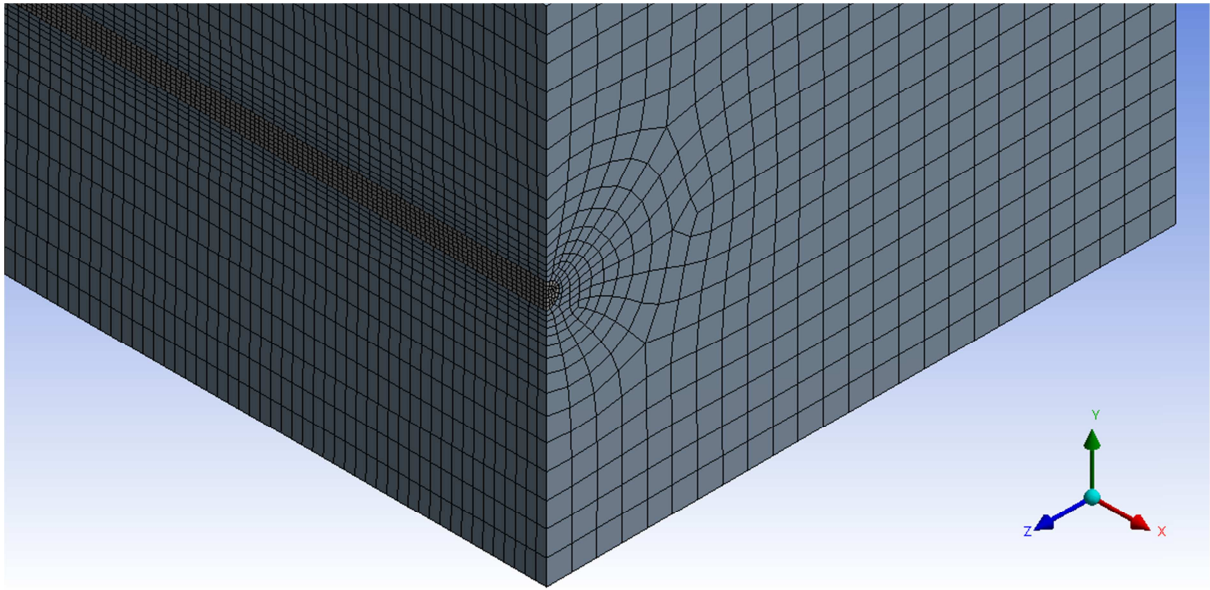


Fig. 1 – A schematic diagram of reservoir-wellbore model



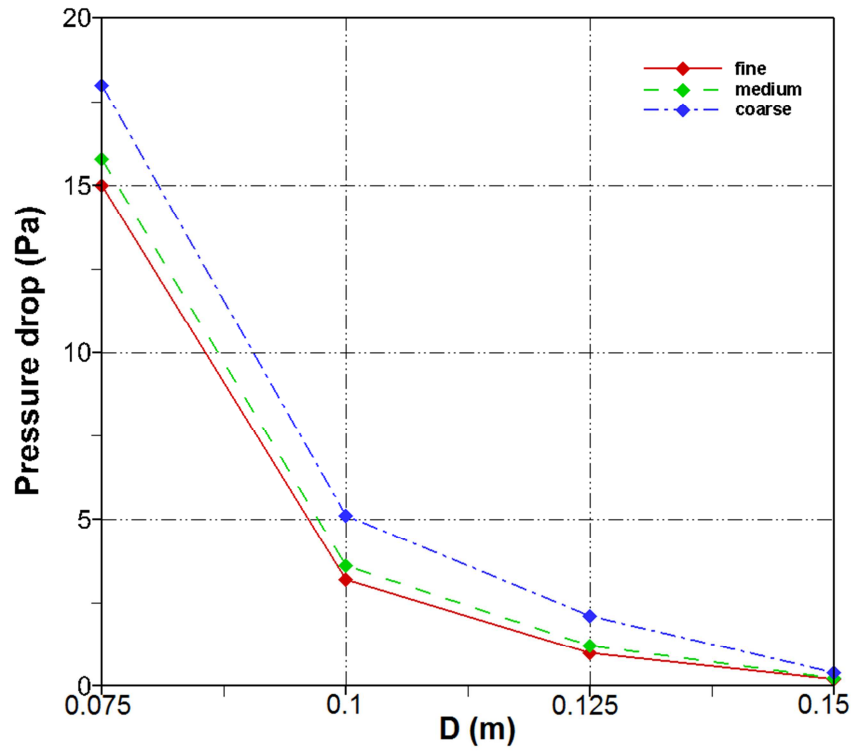
1

2

3

Fig. 2 – Computational mesh of reservoir-wellbore model





1

2

Fig. 3 – Pressure drop vs. wellbore diameter for methane flow with different mesh resolutions

3

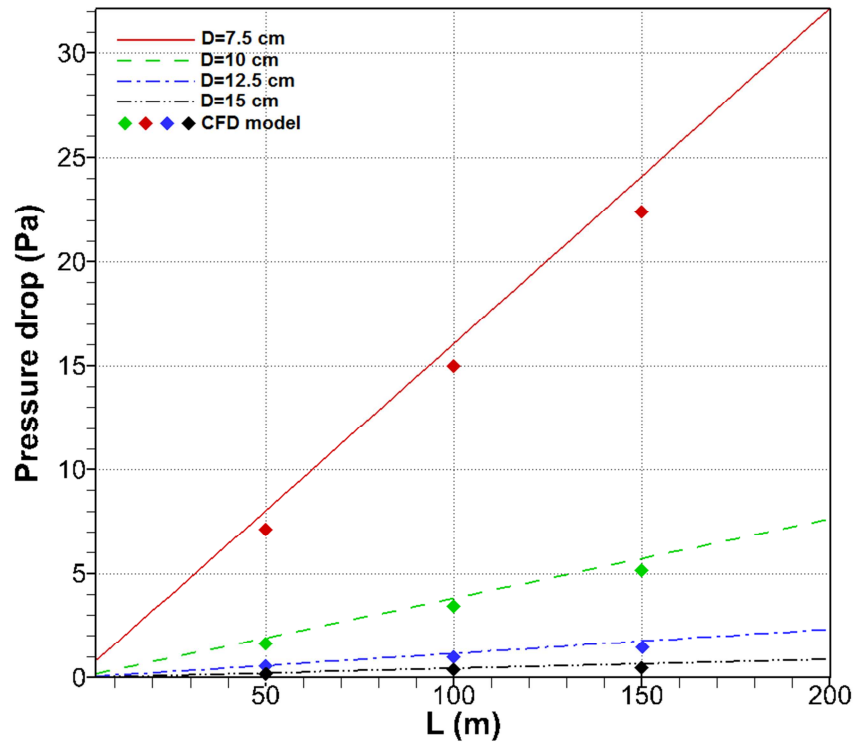


Figure 4 – Comparison of simulated model for methane flow with Atkinson equation (Le Roux, 1990)

1  
2  
3  
4  
5

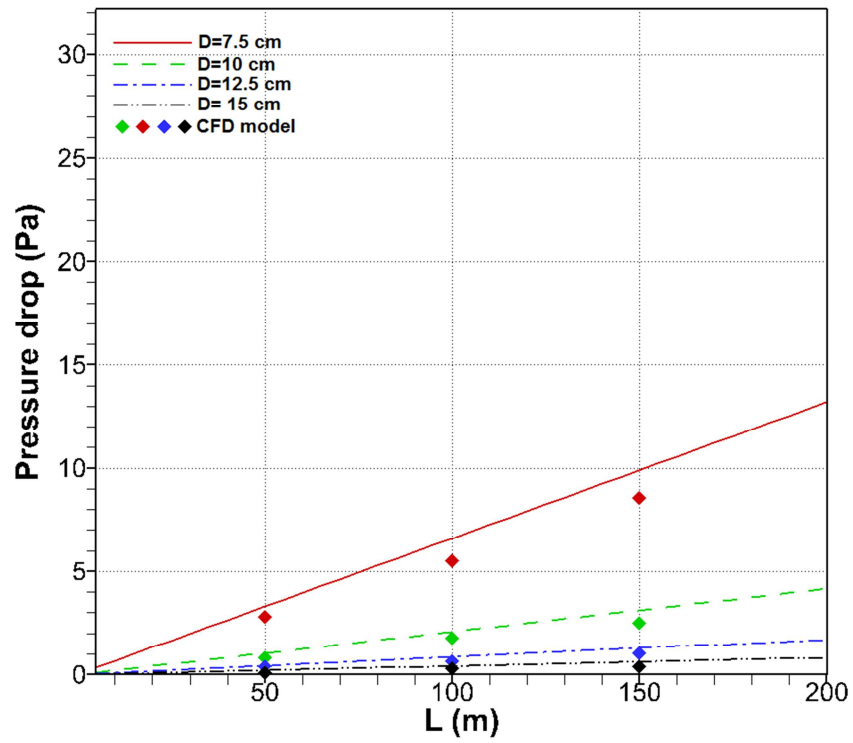


Figure 5 – Comparison of simulated model for water flow with (Aziz and Govier, 1972) correlation

1

2

3

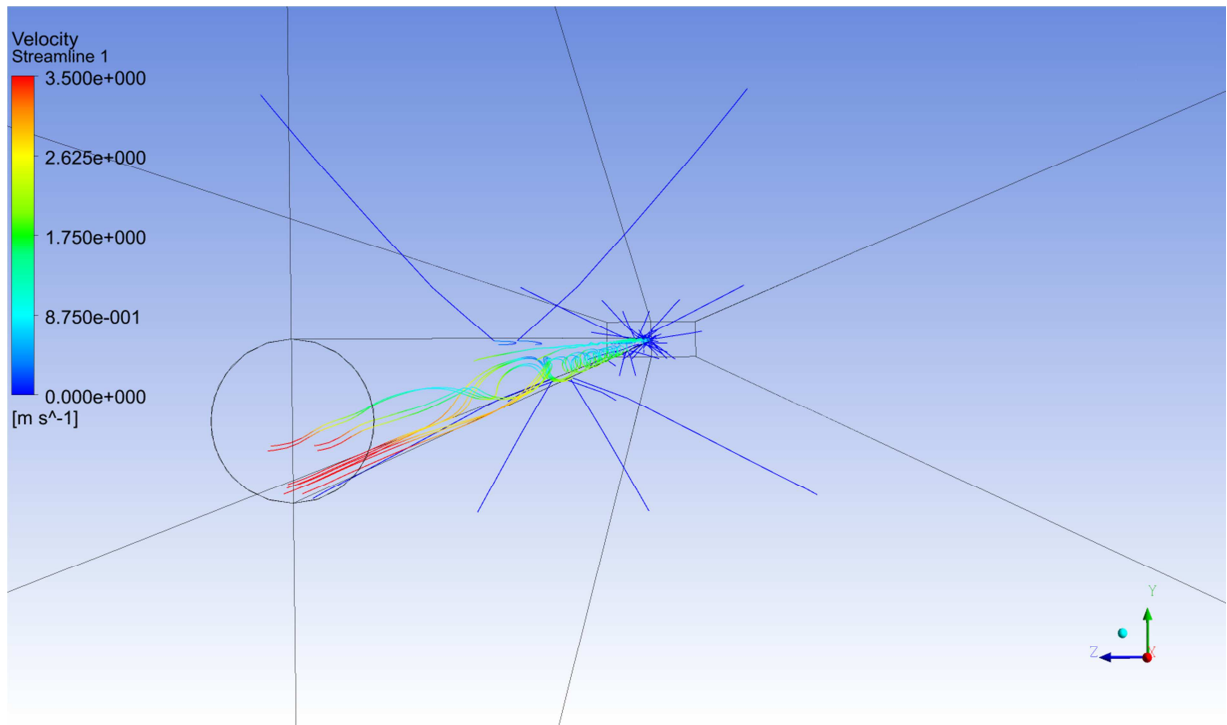
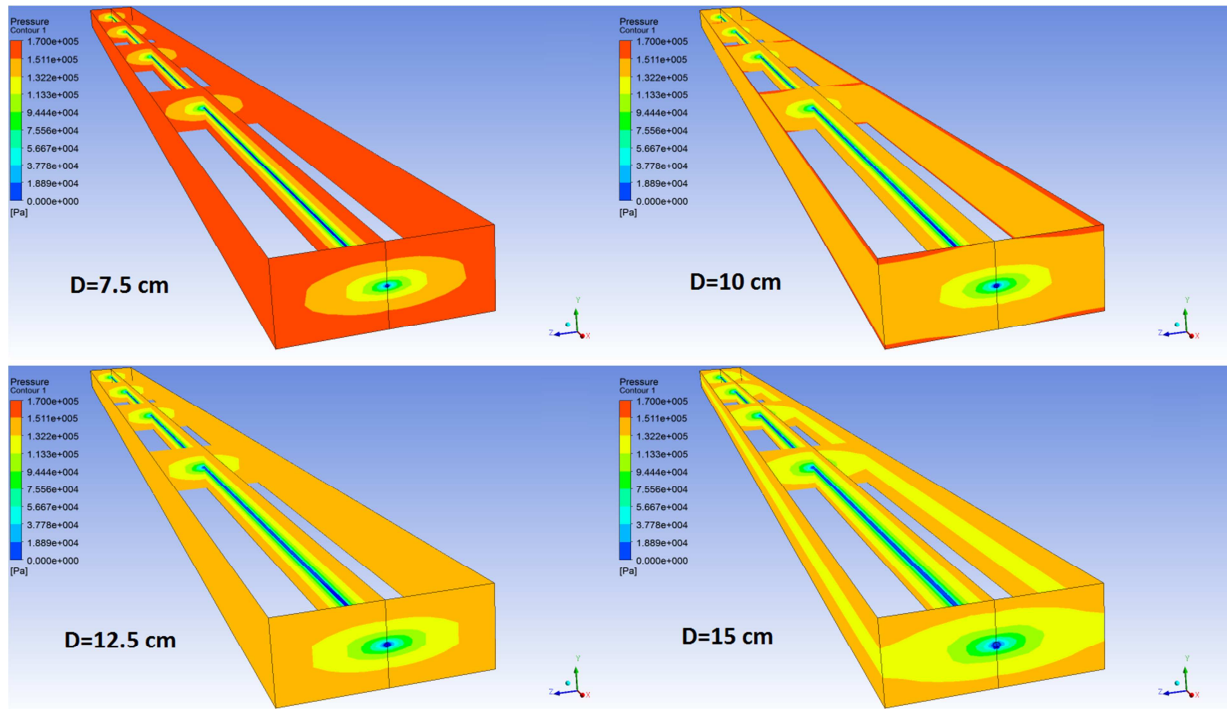


Figure 5 – Velocity streamlines through coal seam reservoir and wellbore

1

2

(a)



(b)

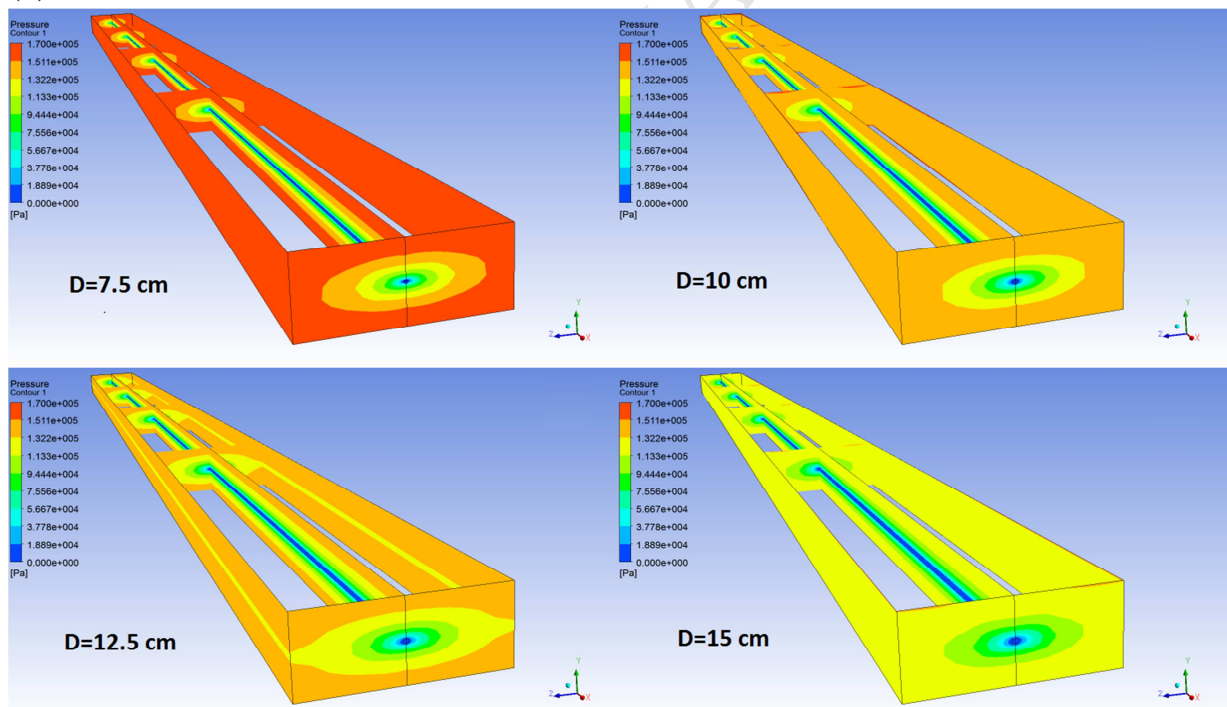
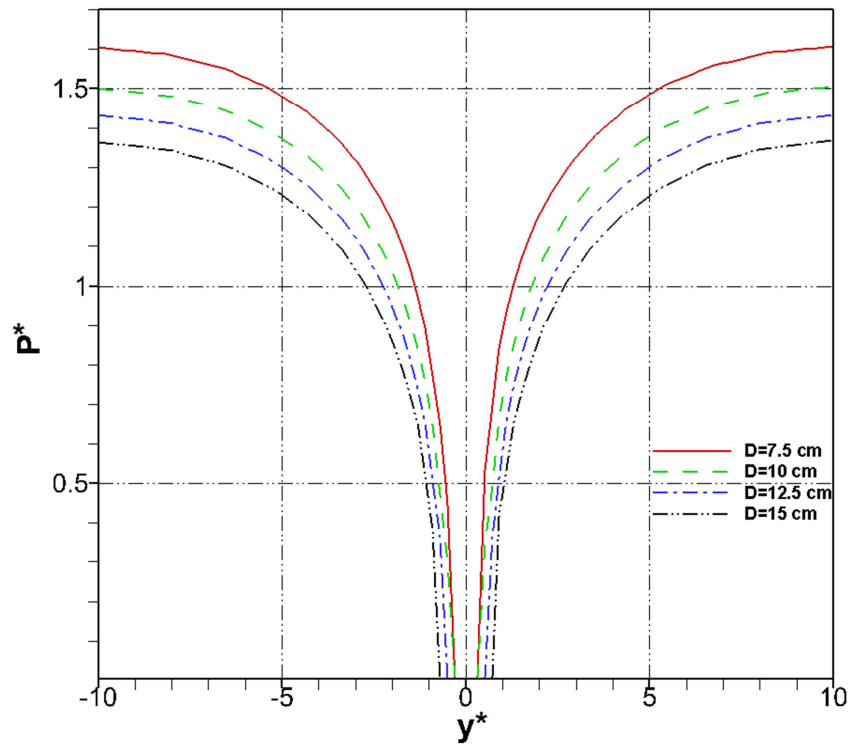


Figure 6 – Pressure contours along coal seam for different wellbore diameters for:  
 a) methane flow, and b) water flow

(a)



(b)

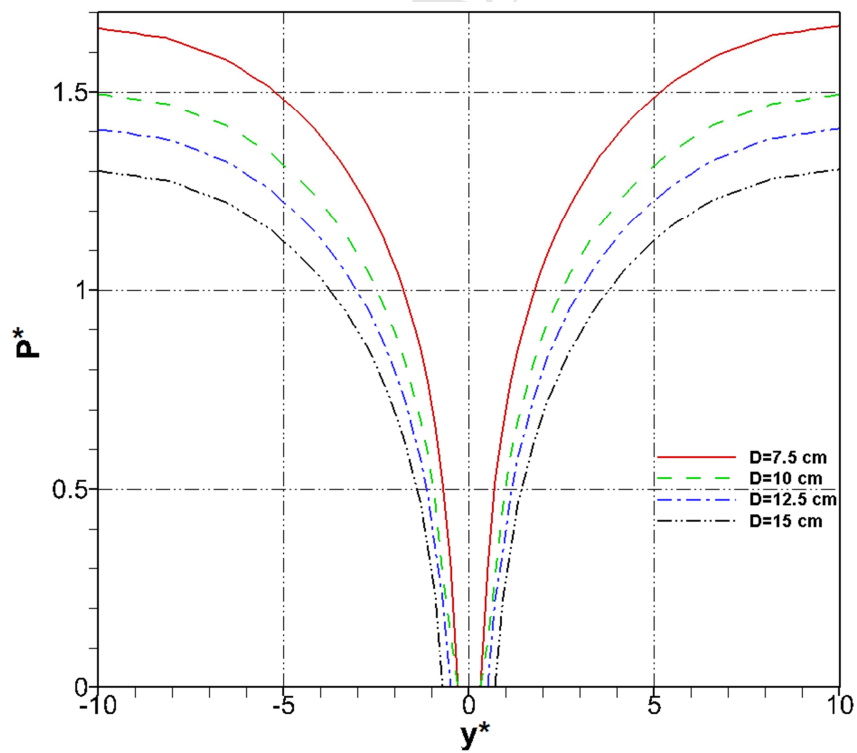
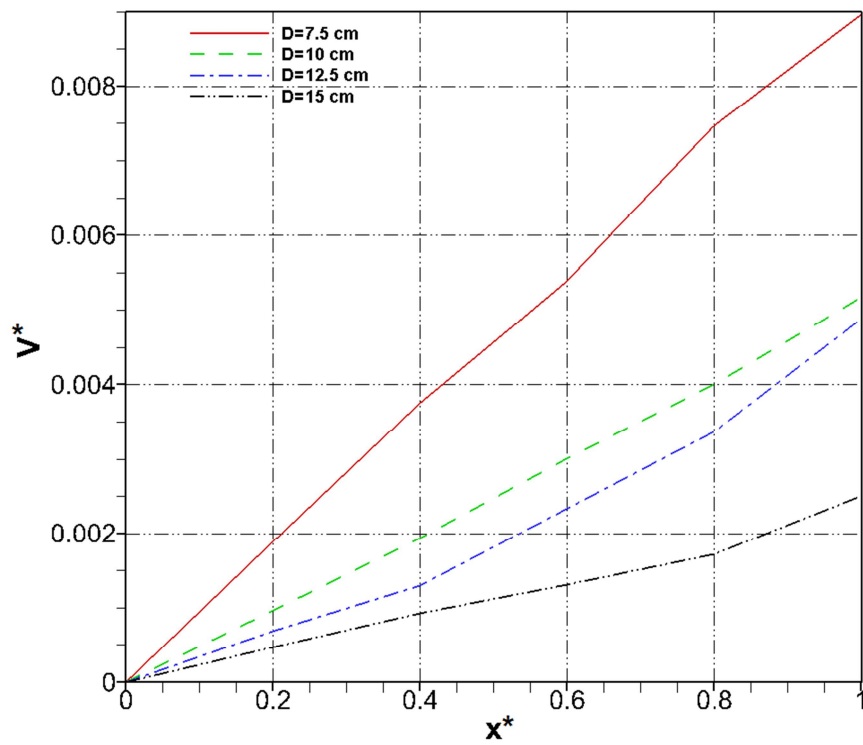


Figure 7 – Pressure distribution in  $y$  direction across coal seam at  $x^* = 0.5$  for: a) methane flow, and b) water flow

(a)



(b)

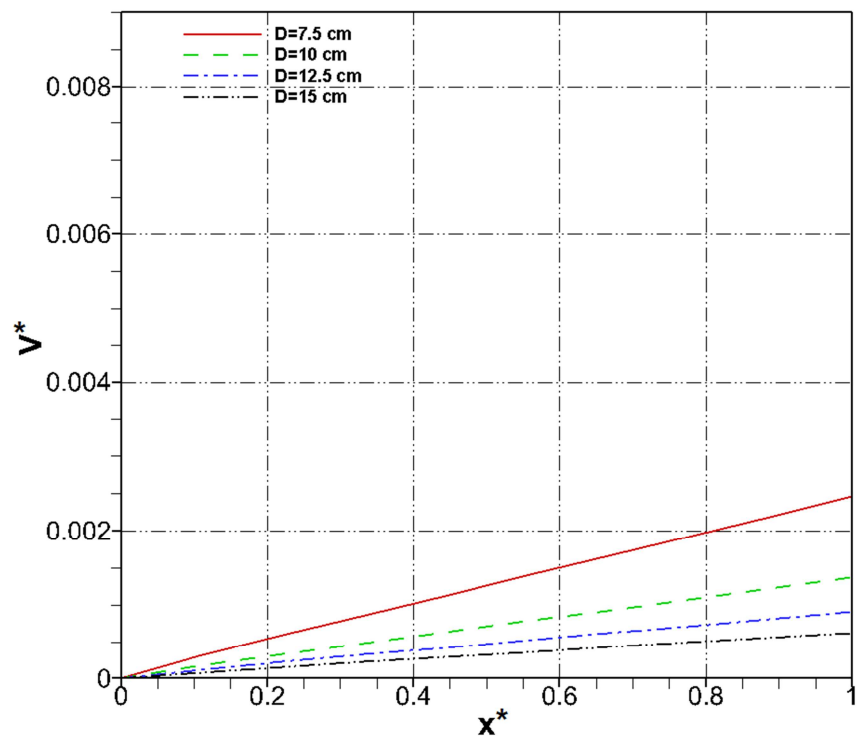


Figure 8 – velocity along wellbore centreline for: a) methane flow, and b) water flow

1

2

3

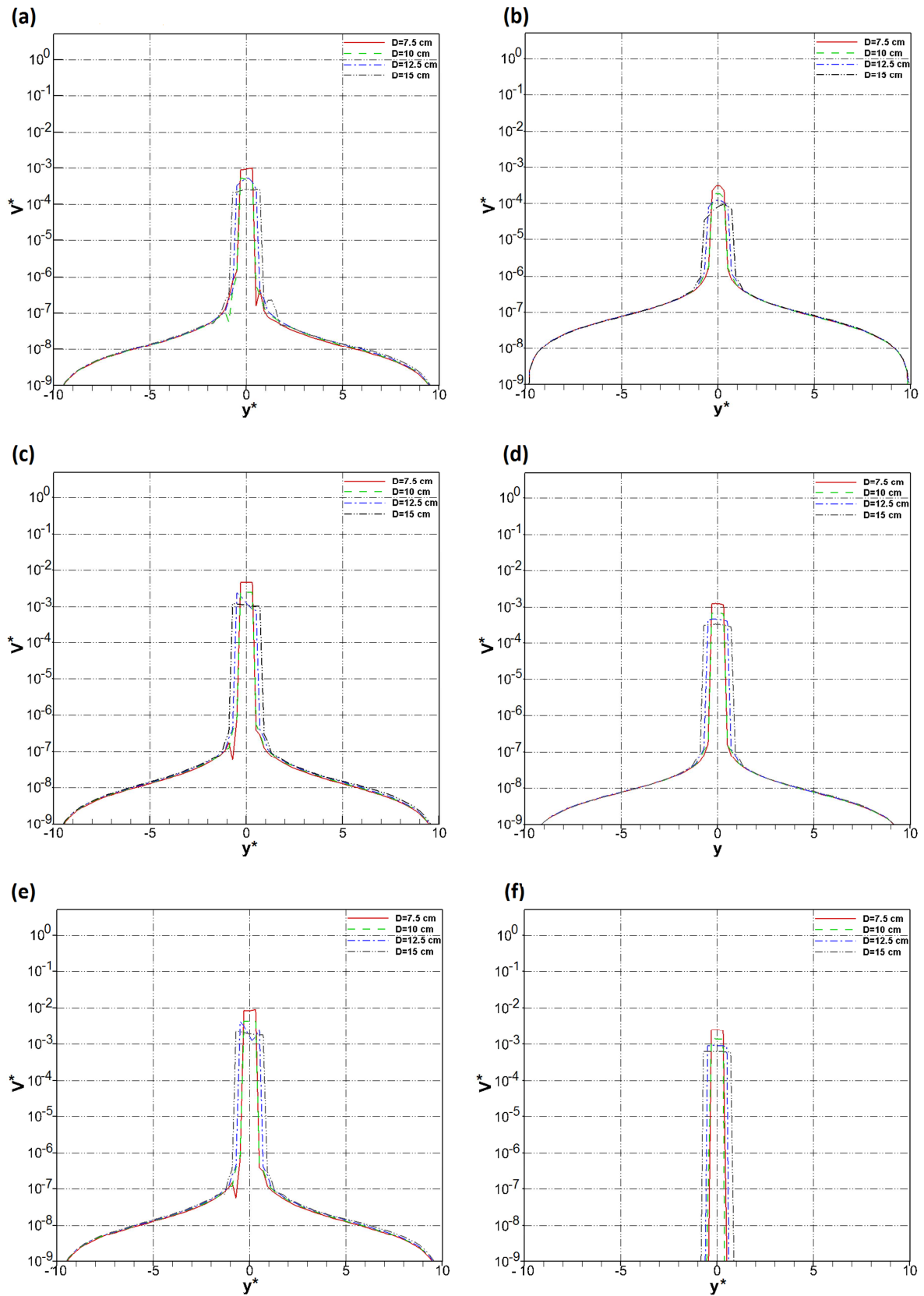


Figure 9 – Velocity profile along Y direction for methane (left) and water (right) flow at: a,c)  $x^* = 0$ ; b,d)  $x^* = 0.5$ ; e,f)  $x^* = 1$



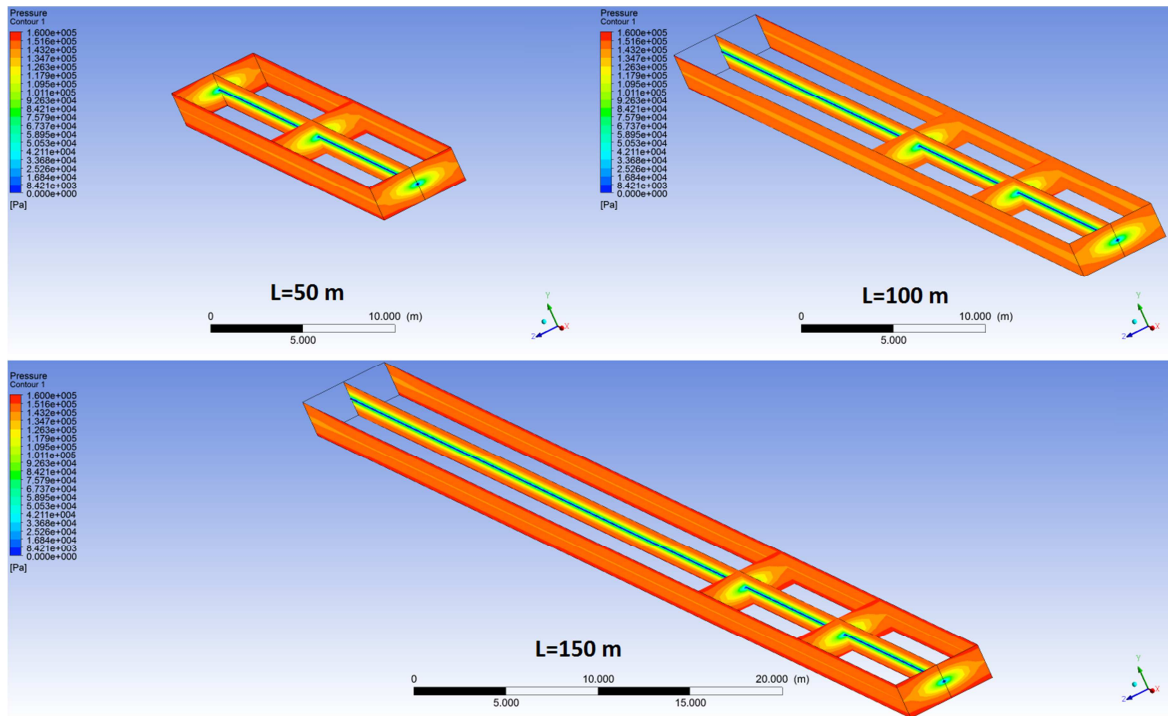
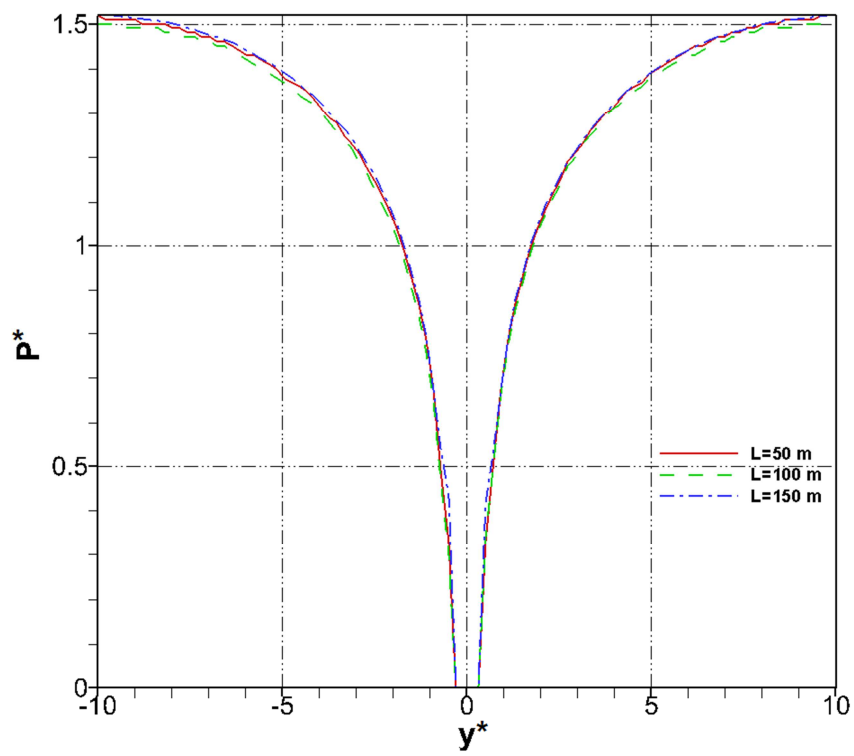


Figure 10 – Pressure contours along coal seam for different wellbore lengths

1  
2  
3

(a)



(b)

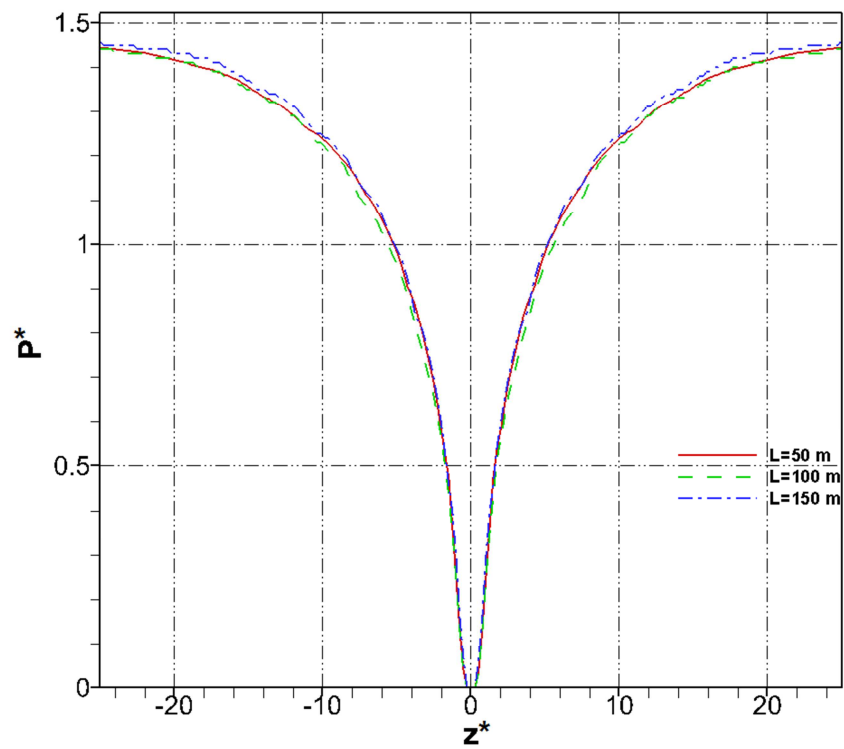


Figure 11– Pressure distribution at distance of 25 m from wellbore outlet in: a) y direction, and b) z direction

1

2

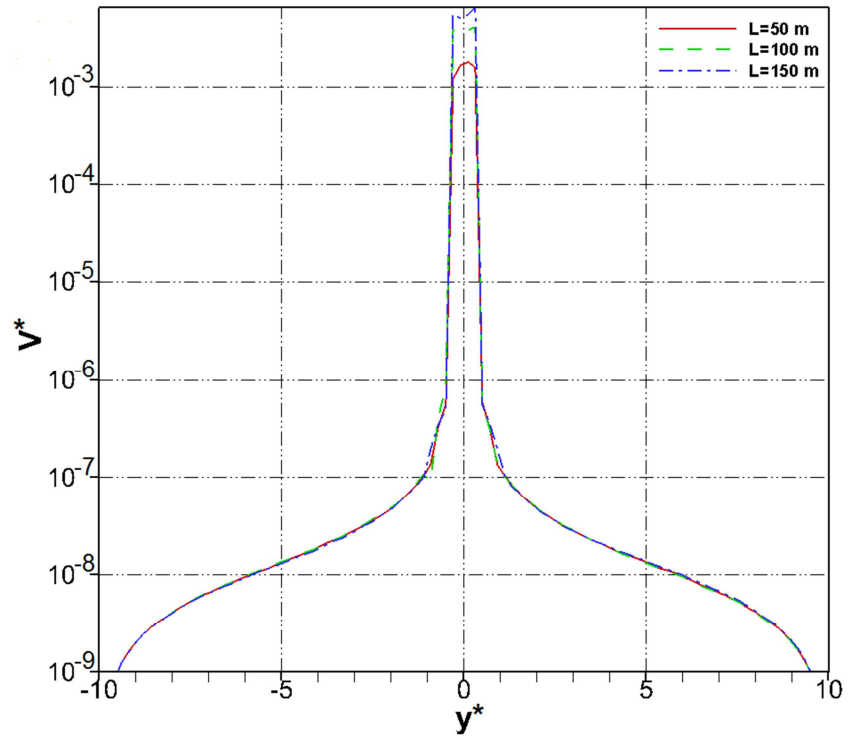
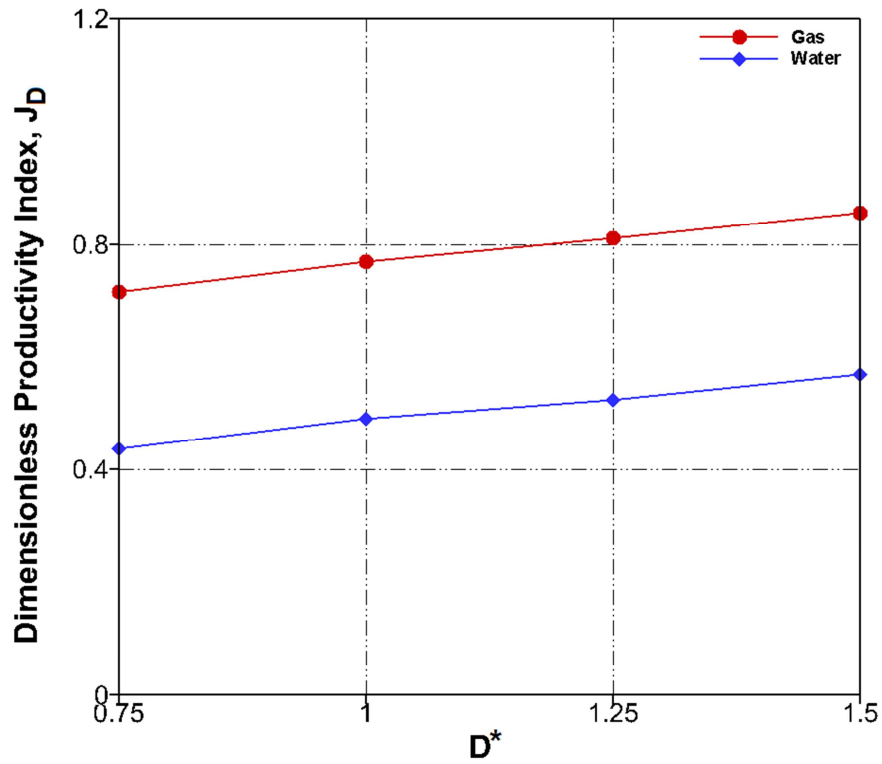


Figure 12 – Velocity profile along  $y$  direction at the distance of 25 m from wellbore outlet for different wellbore lengths

1  
2  
3

(a)



(b)

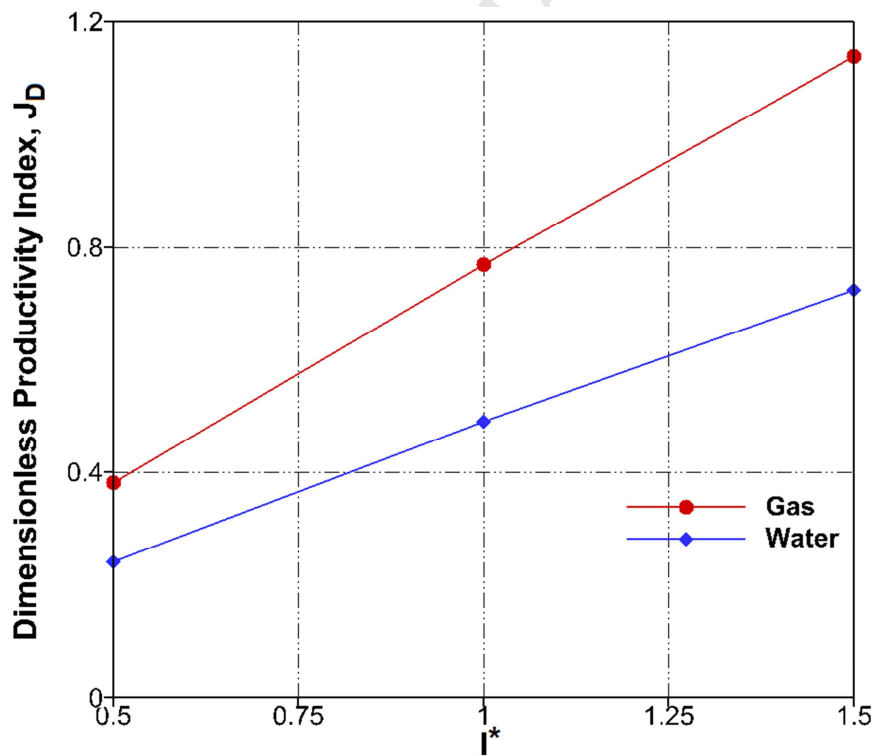


Figure 13 – Productivity index for different wellbore geometries. a) wellbore diameter; b) wellbore length

1

2

1

Table 1. Dimensionless parameters

Variable type	Dimensionless parameters	
Independent variables	$x^* = \frac{x}{L_0}$	$y^* = \frac{y}{D_0}$
	$z^* = \frac{z}{D_0}$	$l^* = \frac{l}{L_0}$
Dependant variables	$V^* = \frac{V}{\sqrt{P_0/\rho_0}}$	$p^* = \frac{p}{p_0}$

2

3

4

Table 2. Comparison of wellbore-only model with integrated reservoir-wellbore model

Wellbore dimensions (m)	Pressure drop (Pa)		Relative error* (%)	
	Reservoir-only	Integrated reservoir-wellbore	Reservoir-only	Integrated reservoir-wellbore
D=0.075, L=100	18.59	15.02	15.7	6.5
D=0.10, L=100	4.77	3.46	25.1	9.2
D=0.125, L=100	1.74	1.07	49.4	8.1
D=0.15, L=100	0.6	0.41	37.9	5.7
D=0.10, L=50	2.45	1.73	28.6	9.2
D=0.10, L=150	6.85	5.28	19.8	7.6

1 \* relative errors are calculated based on Atkinson's equation

**Highlights:**

- An integrated CFD model of reservoir-wellbore flow was developed.
- Fluid production can be enhanced by increasing the wellbore diameter and length.
- Increasing the wellbore diameter leads to pressure reduction through coal seam.
- At a certain distance from wellbore outlet, pressure is independent of upstream flow.